vehicles

MDPI

Article

Chassis Modeling for Driving Behavior Analysis Using 3D Scans

Philip Rautenberg *, Niklas Leonard Ostendorff and Michael Frey

Institute of Vehicle System Technology, Karlsruhe Institute of Technology, 76131 Karlsruhe, Germany; niklas.ostendorff@kit.edu (N.L.O.); michael.frey@kit.edu (M.F.)
* Correspondence: philip.rautenberg@kit.edu

Abstract

Full-vehicle test benches are used for the development and validation of vehicle functions or components. To obtain realistic results, the vehicle's (sub)systems and the surrounding environment must be simulated in a suitable simulation environment on the test bench. One relevant subsystem to many studies is the chassis, which behaves differently on the test bench due to the absence of spatial accelerations. However, the relevant information for simulating the chassis is often known only to the manufacturers. To address this challenge, this publication presents a method for obtaining a reliable kinematic model of the chassis. The chassis is captured using a 3D scanner, allowing relevant hard points to be determined. Using IPGKinematics, wheel travel curves are extracted from these hard points for simulations in CarMaker. The simulation results were validated against real-world driving maneuvers performed with the vehicle under test. The comparison shows a high level of accuracy despite some simplifications in the simulation. The presented method can therefore be considered valid. To further validate the method, various potentials are discussed and possible extensions are presented.

Keywords: chassis; suspension kinematics; suspension; wheel travel; kinematics and compliance; vehicle dynamics; reverse engineering; 3D scanning

1. Introduction

The validation of functions or components in vehicle development is often conducted using X-in-the-loop methods. This ranges from purely software-based analyses to tests involving the entire system. Intermediate steps often consist of a combination of software and hardware in which real components are integrated with a suitable simulation environment to form a complete system. Full-vehicle test benches, which simulate driving resistance forces, address such scenarios. These test benches are used to investigate the vehicle powertrain [1], validate automated driving functions [2], or study vehicle–driver interaction [3].

With full-vehicle test benches, two distinctions are generally made. The first distinction is made between roller, flat-track, and powertrain test benches. The second is between test benches with or without steering functionality. In the case of roller and flat-track test benches, the vehicle is present entirely and is either mounted on rollers or a flat track. In contrast, on powertrain test benches, the tires are removed, the wheel hub is connected directly to a load unit, and the tire behavior is simulated. Powertrain test benches also often allow for steering maneuvers to be performed without modifying the vehicle, thereby enabling the investigation of lateral dynamic driving situations. In some cases, this is also possible on roller or flat-track test benches [4]. However, the vehicle's steering system

Check for updates

Academic Editor: Pak Kin Wong

Received: 28 September 2026
Revised: 22 October 2026
Accepted: 23 October 2026
Published: 2 November 2026

Copyright: © 2026 by the authors. Licensee MDPI, Basel, Switzerland. This article is an open access article distributed under the terms and conditions of the Creative Commons Attribution (CC BY) license.

is usually simply disconnected and stimulated using emulators to implement steering functions [5,6]. Further details on the various test bench configurations can be found in [7].

A test bench for simulating driving behavior that operates according to the principle of a powertrain test bench is the vehicle-in-the-loop (ViL) full-vehicle test bench at the Institute for Vehicle System Technology at the Karlsruhe Institute of Technology (KIT). In addition to the drive torque for each individual wheel and the wheel speeds, the test bench examines the wheel steering angles and the wheel aligning torque. Thus, the vehicle's drivetrain and steering system can be analyzed. All the other components and subsystems as well as the environment are simulated in the software CarMaker Testbed 14.1. Details about the test bench can be found in [1–3,8]. Figure 1 shows the ViL test bench, including the device under test (DUT).



Figure 1. The KIT's ViL full-vehicle test bench, which is used as the target application for the objective of this paper.

The common feature of these full-vehicle test benches is the absence of spatial acceleration of the vehicle. Although the vehicle body moves due to the suspension kinematics during steering maneuvers or the support of the traction forces on the suspension, this body motion differs from that on the road [8]. Only a few test benches are equipped with an additional mechanism that is capable of further accelerating the vehicle body [9,10]. In all cases, however, the suspension kinematics must be known so that the correct body accelerations can be applied or, at a minimum, the influence of the vehicle body movements and the associated wheel load shifts on driving dynamics can be taken into account. The suspension kinematics can be determined either from the suspension's computer-aided design (CAD) data or by measuring a vehicle on an axle kinematics test bench, also known as a kinematics and compliance (K&C) test bench. The use of K&C test benches involves high costs, and CAD data is usually only accessible to vehicle manufacturers.

This latter challenge often arises in other areas of vehicle development as well. One solution for preserving CAD data is three-dimensional (3D) scanning of components. High-density point clouds make it possible to map surfaces, particularly the increasingly common free-form surfaces that cannot be reduced to simple geometric shapes. This technology is already being used in various applications in vehicle development [11,12] and other areas of engineering [13]. However, in many cases, only design spaces or disassembled individual components are scanned, and the entire system or installed components are rarely scanned. Previous approaches focusing on the chassis application have involved scanning individual components [12,14,15] or a chassis frame [16].

The challenge lies in the need to measure the installed chassis rather than the removed individual components since, otherwise, among other things, the parameters of the wheel travel kinematics cannot be determined. Measuring assembled components is challenging because the available space for moving the scanner around the suspension is limited while still requiring a complete capture of all the relevant kinematic points—also known as hard points—of the chassis. Without a complete capture of the chassis, the hard points cannot be extracted, nor can a chassis model be generated from them.

A comprehensive method for scanning an entire chassis and creating a chassis model from the scan data is not yet known and is the objective of this publication.

2. Fundamentals and State of the Art

2.1. Chassis and Relevant Parameters

According to the authors in [17], the chassis can be subdivided into three components: a powertrain mounting, an axle module, and tires/wheels. The axle module consists of the axle drive, stabilizer bar, steering system, chassis subframe, suspension, and wheel brake modules. For the purposes of this paper, a detailed examination of the suspension and steering system is necessary. The suspension includes, among other components, control arms, knuckle-pins, wheel carriers, the spring-damper system, as well as bearings and joints. The steering system essentially comprises the tie rod and the steering transmission. The entire system of these individual assemblies and components connects the vehicle body to the road surface and is primarily responsible for driving dynamics, stability, and comfort.

By arranging the aforementioned assemblies and individual components in different ways, various chassis designs can be implemented. Essentially, a distinction is made between rigid and semi-rigid axles, as well as independent suspensions. These are subdivided into a total of over 20 different individual designs.

The arrangement of the individual components results in various parameters of wheel travel and steering kinematics, which vary depending on the exact design of the components. These parameters can be categorized into angles (e.g., toe-in or camber), radii, instantaneous centers of rotation, and axes of motion. For a detailed explanation of a chassis structure, its individual components, suspension types, and parameters, refer to [17–19].

2.2. Methods for Chassis Analysis

A chassis can be analyzed in various ways. These methods can be divided into theoretical and practical approaches. The theoretical methods include analysis using CAD models and conducting simulations with appropriate chassis behavior models. The behavioral models are primarily based on spatial multi-body systems (MBS) in which rigid bodies are represented as mass points and their relationships to each other are modeled using joints. Calculating the acting forces or the dynamics of the resulting entire system is computationally intensive as differential equations must be solved.

There are multiple vehicle-dynamic-specific MBS software solutions. Software like Adams Car, IPGKinematics, Race, and SuspensionSim are all examples of MBS simulation

software that provide a limited but vehicle-specific (simulation) environment. After the initial setup of the MBS, these programs run virtual K&C cycles to determine the behavior for parallel and reciprocal rebound and compression as well as during steering.

A less computationally intensive alternative is the use of characteristic curves derived from MBS simulations. However, this results in lower model accuracy. A requirement for such theoretical investigations is access to or knowledge of the construction data. Details on the simulation of a chassis can be found in [20].

A practical chassis analysis approach involves performing driving maneuvers with a real vehicle on test tracks. In addition to a vehicle, this requires appropriate measurement equipment. The more measurement equipment installed on the vehicle, the more accurately the chassis can be analyzed. However, at least one inertial measurement unit (IMU) is required to evaluate the vehicle's handling based on the measured accelerations. The challenge here is the respective increase in effort, and thus costs, when a high level of accuracy is required.

A less time-consuming but still cost-intensive practical method is the use of K&C test benches, like in [21]. Such test benches are used to measure the kinematic and elastokinematic parameters of the chassis. In this process, the vehicle body is fixed in place and the wheels or wheel hubs are attached to actuators. The actuators apply forces in all spatial directions, and the movement and resistance of the chassis are measured. The measured parameters include, among others, the displacement of the wheel contact points and wheel centers, changes in toe, camber, and caster angles, and the steering ratio. Furthermore, the roll poles can be calculated. The relative motion between the wheels and the body allows for the measurement of changes in axle kinematics, as well as the forces and stiffnesses of the chassis. To measure the kinematics, the wheels are compressed and extended simultaneously and alternately. To measure the elastokinematic influence, longitudinal and lateral forces are applied to the tires. The K&C test bench is considered as the standard for determining the kinematics and elastokinematics of a vehicle [17]. These test benches are essential for vehicle development and are used for chassis development, chassis adjustment, and driving dynamics simulation [22].

3. Materials and Methods

3.1. Device Under Test

The DUT, mounted on the ViL test bench as shown in Figure 1, is a Hyundai Ioniq 5. The relevant technical specifications of the battery electric vehicle are listed in Table 1. The listed center of gravity (COG) position was determined in advance using a COG measurement method and refers to the contact point of the front left wheel. For a correct calculation of the COG, the COG was measured with the weight equivalent of two occupants placed in the DUT. Furthermore, the DUT was equipped with a variety of measurement devices at the time of the test. Using this measurement equipment, the DUT's steering angle could be read, allowing the DUT to be aligned straight for the scanning process.

The DUT has a McPherson strut with an L-shaped control arm on the front axle. A multi-link suspension is installed on the rear axle. The spring and damper are separate on the rear axle and are both mounted on the lower control arm.

Table 1. Technical specifications of the DUT.

Description	Data
Wheelbase	3 m
Track width	1.65 m
Vehicle weight	2460 kg
COG in x-direction	−1.565 m
COG in y-direction	−0.8284 m
COG in z-direction	0.6009 m

3.2. Scanning Tools

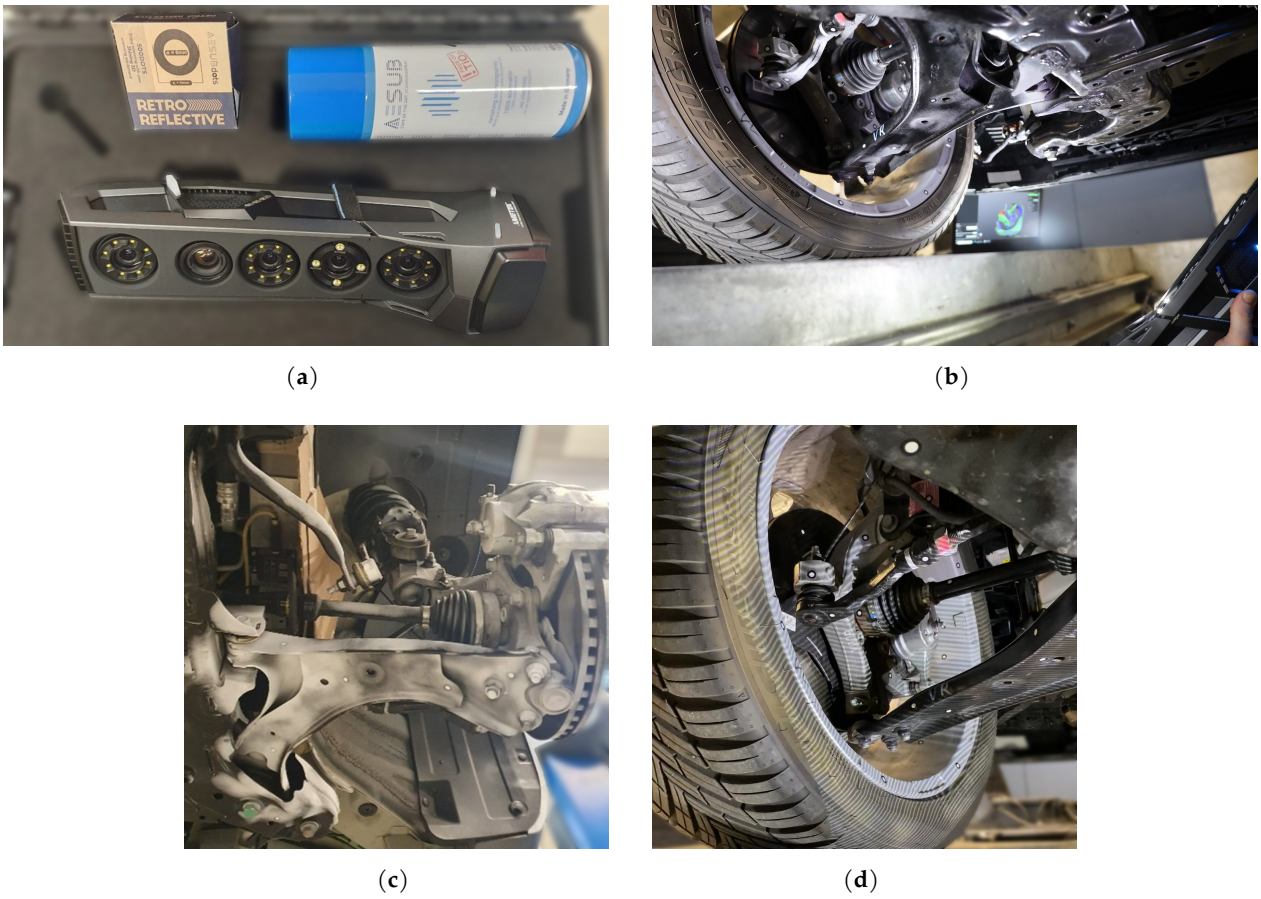
The 3D scanner used in this publication is the Go!SCAN 3D structured-light 3D scanner from Creaform; see Figure 2a. The scanner's technical specifications are listed in Table 2.

Table 2. Technical specifications of the Go!SCAN 3D [23].

Description	Data
Accuracy	0.05 mm
Volumetric accuracy	0.15 mm/m
Measurement resolution	0.1 mm
Measurement rate	1,500,000 measurements/s
Recommended part size range	0.1 m to 4 m

The scanner operates on the principle of the structured light projection method. In this process, a high-contrast stripe pattern is projected onto the object and simultaneously captured by two cameras. The surface can be calculated based on the distortion of the stripes on the surface caused by inclines and curves. The stripe pattern from the scanner used on the chassis of the DUT is shown in Figure 2d. The scanner—or its generated stripe pattern—is guided over the object to be scanned using slow and steady movements. The individual measurement points form a dense point cloud from which a surface model is generated. This data processing takes place in the software suite VXelements 12, which is also offered by Creaform. The software consists of several workbenches. The VXscan module is used for the scanning process. The VXmodel module can be used afterwards to post-process the surface geometry, for example, to create design elements. The design elements can be derived from the scanned geometry by selecting a surface, individual facets, or points. The selection of a surface can be specified, for example by angle or continuity, in order to isolate the correct geometry. Other reverse engineering software like Artec Studio from Artec 3D may also be used. Further software solutions for processing the scans or post-processing as well as other scanners are listed in [13].

In addition to the scanner, a special scanning spray and retro-reflective adhesive dots are used, which are also shown in Figure 2a. The scanning spray creates a matte-reflective surface to improve the scanning of dark or highly reflective surfaces, as shown in Figure 2c. The adhesive dots further increase the accuracy of the scan by serving as reference points for image processing. Individual adhesive dots can be seen, among other places, on the rim flange in Figure 2b.



(**a**) (**b**)

(**c**) (**d**)

Figure 2. Overview of the scanning tools and the application: (**a**) 3D scanner Go!SCAN (bottom), retroreflective dots (left) and scan spray (right). (**b**) The scanner (bottom right) during a scan of the front axle with the software VXscan running in the background (center). (**c**) Wheel suspension prepared for 3D scanning with the scan spray. (**d**) Visualization of the projected light strips on the wheel suspension.

3.3. Chassis Modeling Method

This chapter presents the methodology for digitizing the hard points and the subsequent calculation of the wheel travel. The first subsection outlines the preparation of the vehicle for the scan process, the steps for the scan and post-processing to extract hard point coordinates. The following subsection explains using the extracted coordinates to calculate the wheel travel dynamics for further use in a simulation environment. Since the wheel travel dynamics is to be used on the ViL full-vehicle test bench, where CarMaker Testbed 14.1 is implemented, IPGKinematics 3.6.11 is used as the MBS environment to simplify the transfer.

3.3.1. From Real Parts to CAD: Chassis Scanning

To perform a chassis scan for the aim of digitizing the hard points, the DUT must first be prepared. Therefore, weights need to be added to the vehicle to simulate the given design attitude or the setup for which the simulation model is being created so that the COG matches. For improved access to the chassis with the scanner while maintaining the vehicle's design attitude the DUT is driven over an inspection pit. Performing the scan on a car lift with removed wheels improves the access to the chassis compared to an inspection pit. However, since on a car lift the wheels become unloaded and rebound, the design attitude is not being kept, thus limiting the usefulness of this method. Nevertheless, a car

lift can be used as an additional step to improve the scan of the body-mounted joints and increase the accuracy of the nodes if the scan is used to complement the primary scan.

Using the inspection pit, the last few meters should be driven without a steering input so that the wheels can align themselves. Fairings and control arm covers that limit the scanning range also need to be removed beforehand. As described in Section 3.2, a scanning spray is applied to all surfaces that need to be scanned. Retro-reflective dots are also applied at random distances from each other and with a sufficient density so that the scanner has at least three points in its field of view for every angle at which the scanner is held while maintaining the correct distance to the parts.

The chassis can then be scanned with a slow and gentle sweep of the scanner while maintaining the proper distance to the surface, which is indicated by a status light on the scanner. The generated point cloud can be inspected in VXscan. If the scan is partially of low quality or incomplete, the scan can be paused, scanning spray and dots can be added if necessary, and the scan can be resumed. To help tracking and merging the scans the area that is to be re-scanned can be selected in VXscan, also showing the position the scanner needs to be held at to match the selection. This process is the same for each axle.

If the scan is complete, satisfactory, and of sufficient quality, respectively, the 3D scan data needs to be cleaned up by removing noise and floating data as well as unnecessary surfaces. Those steps improve the responsiveness of the model and performance of the tools used to identify the hard points. Basic geometric shapes, most notably cylinders, and construction elements like planes, axes and points can be fitted to a surface selection and their intersections can be used to locate the hard points of the joints of the chassis. This procedure needs to be applied to all joints until a node for every necessary hard point is created. If hard points cannot be located using the given surfaces, due to them being incomplete, for example, estimates and manual measurements of the vehicle need to be completed to approximate their location. The coordinates of each node need to be read out and transformed so that their coordinate origin coincides with the COG as this is used as the universal reference point. Alternatively, the coordinate origin of the scan can be set to another preferred reference point during the dataset preparation. For this step any spreadsheet editor may be used.

3.3.2. From CAD to Simulation: Suspension Kinematics

The determined coordinates can then be entered into MBS software as IPGKinematics. Within IPGKinematics the kinematics and compliance of a chassis can be calculated like the suspension kinematics during compression, rebound and steering. The two interfaces needed for the calculation are *Simulation Control* and *Vehicle Data*. Within the Simulation Control interface, the step size and range of motion for which the chassis geometry is calculated can be set. The interface for Vehicle Data input has five index tabs, namely *General, Springing, Bushings, Mass, and Geometry*. For a purely kinematic calculation, also referred to as a "Forces Off simulation" [24], only the General and Geometry tabs are needed. Therefore, the chassis subframe toggle in the General tab, shown in Figure 3, needs to be disabled. Within the General tab basic information about the vehicle and axle can be defined, while the coordinates of each hard point are defined in the Geometry tab. The hard points for a McPherson strut suspension in the Geometry tab are listed in Table 3. For each hard point x-, y-, and z-coordinates are required. Note that, for a "Forces Off simulation" the nodes for bushings, springs and dampers, as well as the axles, are generally not taken into account, but they do need a non-zero value to not produce mathematical errors during the simulation. The McPherson strut is an outlier in itself in this regard because the strut, defined by the damper/dashpot shock absorber nodes, functions as wheel guidance and the corresponding nodes are thus needed. The Geometry tab also includes coordinates for

lateral leaf springs, which can be omitted if they are not turned on in the Springing tab. The last entry in the Geometry tab includes the position of the front fender on the horizontal plane as well as the turning radius.

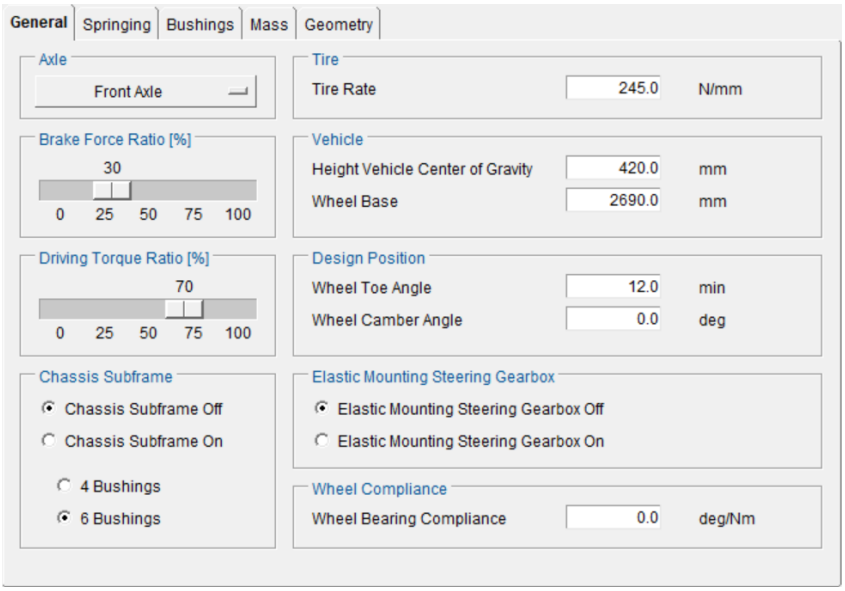


Figure 3. General vehicle and axle information tab in IPGKinematics' Input Data Window with exemplary data.

Table 3. For a "Forces Off simulation" relevant hard points grouped by subsystem.

Subsystems	**Node/Chassis Component**		
Body	Subframe front	Subframe rear	Subframe middle
Wheel	Center	Tire contact point	Force application point
Wheel carrier	Lower wishbone	Damper piston	Steering tie rod
Control arm	Subframe front	Subframe rear	
Axle drive shaft	Differential	Wheel	
Damper	Body	Wheel suspension	
Spring	Body	Wheel suspension	
Strut bushing	Body		
Stabilizer bar	Subframe	Wheel suspension	Stabilizer link
Steering transmission	Body	Steering rod	

To calculate the compliance of the chassis, forces and inertia are also taken into account, requiring an input in the remaining three tabs of the Vehicle Data interface. Within the Springing tab, springs, stabilizer bars, and optional push/pull rods can be defined, either linear or as a curve with up to 15 data points. The Bushings tab enables entering the geometrical location and orientation as well as the stiffness in each axis direction as a proprietary file format. In the Mass tab, mass values for each chassis part can be entered.

Before the wheel travel curves are calculated the chassis geometry resulting from the entered coordinates can be visually inspected in the *Geometrical Control* interface of IPGKinematics.

Last, the file generated by IPGKinematics is imported into CarMaker to emulate the chassis movement, while additional models of the dynamic components like the spring, damper, anti-roll bars, and tires enable a more comprehensive MBS simulation.

4. Results

4.1. Scan Results

After successfully performing the scan following the procedure described in Section 3.3.1, the scan is being prepared by automatically cleaning the point cloud and removing out-of-scope surfaces. Reverse engineering tools or features can then be used to create cylinders, planes, and axes, which conform to the surface selection of wheels, bushing, springs, shock absorbers, joints, and the ground surface. By either directly picking the start, end, or midpoint of a cylinder axis or creating intersections, nodes that represent the hard points can be created.

The scan results for the front axle are shown in Figure 4 and for the rear axle in Figure 5. The added cylinders have been color-coded to group them by domain (i.e., wheel, body, linkages, or suspension strut) in both figures.

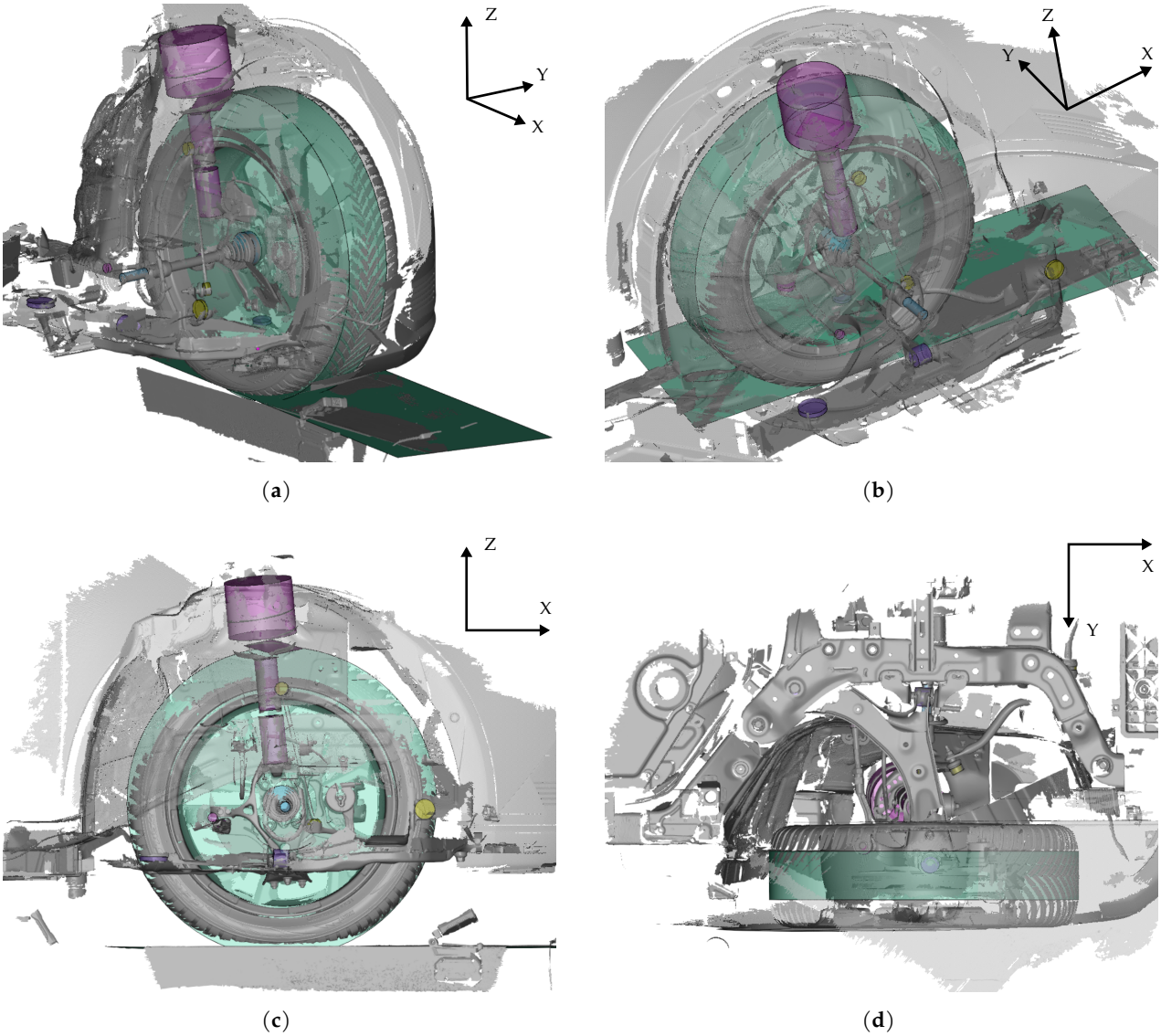


Figure 4. Scan of the front left wheel with added cylinders to represent bushings (purple), coilover (magenta), drive axle (blue), and stabilizer bar joints (yellow) from four different angles: (**a**) angled front view; (**b**) angled view from instrument board; (**c**) right side view; (**d**) bottom view.

Figure 4d displays the bottom view in which the visibility of the lower control arm's front bushing is easily recognizable and as such properly digitized, while the rear bushing of the same control arm is not accessible with the scanner and a mounted wheel. A closer

examination of the scans in Figures 4 and 5 reveals that not all of the required components on both the front and rear axles can be scanned accurately, and therefore assumptions must be made to determine the relevant hard points.

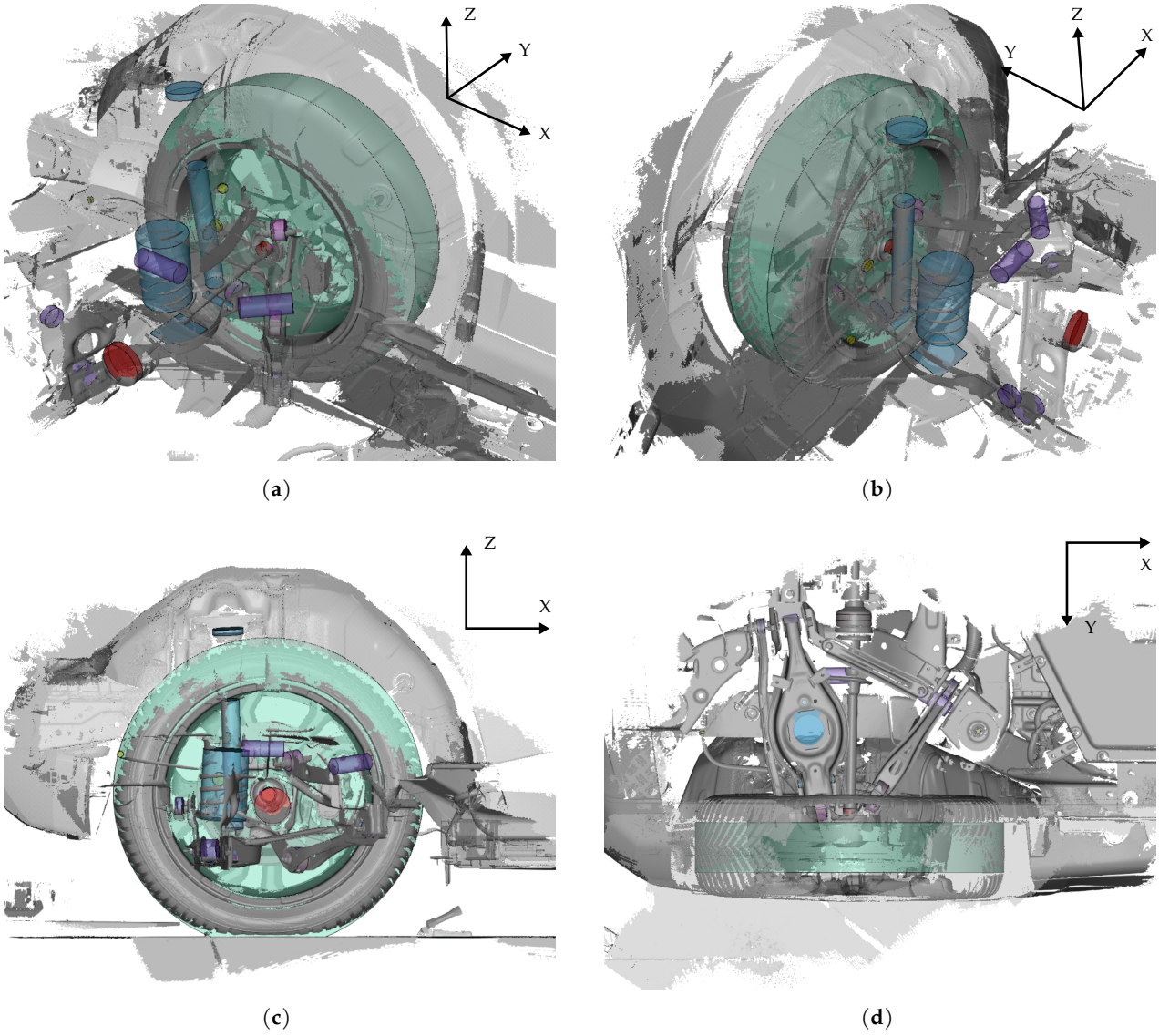
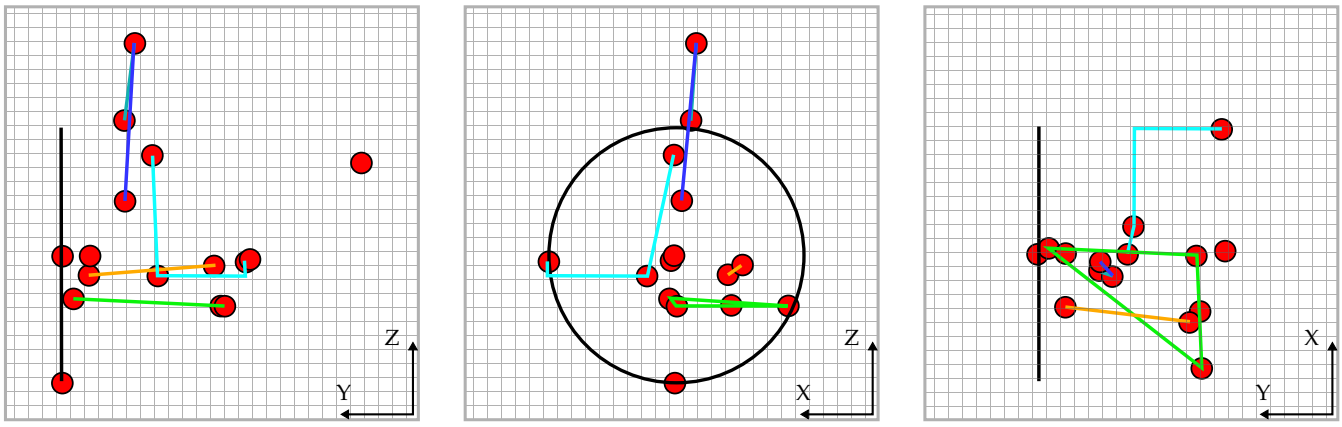


Figure 5. Scan of the rear left wheel with added cylinders to represent bushings (purple), drive axle (red), and stabilizer bar joints (yellow) as well as springs, shock absorber and strut bearing (blue) from four different angles: (**a**) angled view from inside; (**b**) angled view from behind; (**c**) right side view; (**d**) bottom view.

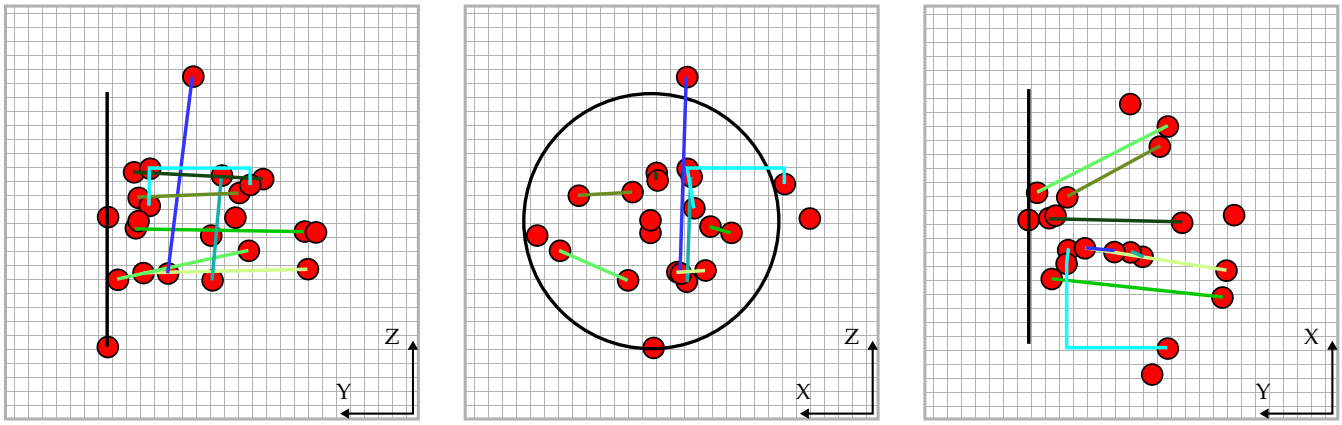
4.2. Transfer to IPGKinematics

In the next step, the determined coordinates are then transferred to IPGKinematics for calculating the chassis kinematic behavior. Since an entire kinematics and compliance simulation within IPGKinematics would require detailed technical information, which can be identified either by the disassembly of all the suspension parts and their measurements or detailed documentation with technical specifications for each part, only the kinematic behavior is calculated, also known as a "Forces Off simulation". Simplified representations of the coordinates of the front and rear axles are shown in Figures 6 and 7, inspired by the Geometrical Control interface from IPGKinematics. Accordingly, relevant components of the chassis are color-coded, and the tires are also shown in a simplified form.



(**a**) (**b**) (**c**)

Figure 6. Geometric view of one front axle suspension for analyzing the determined coordinates and resulting positions of the wheel (black), control arms (green), steering tie rod (orange), stabilizer bar (light blue), spring (turquoise), and damper (blue) from three orthogonal views: (**a**) driving direction view; (**b**) side view; (**c**) bird's eye view.



(**a**) (**b**) (**c**)

Figure 7. Geometric view of one rear axle suspension for analyzing the determined coordinates and resulting positions of the wheel (black), control arms (various shades of green), stabilizer bar (light blue), spring (turquoise), and damper (blue) from three orthogonal views: (**a**) driving direction view; (**b**) side view; (**c**) bird's eye view.

Hard points determined manually could only be identified with limited accuracy. Theoretically, a hard point can be determined via the console contour and/or the position of the through-bolt. However, due to elasticities and wear within the console, such as in the rubber bushings, an estimated hard point can shift by a few millimeters. Based on experience, this displacement can be limited to a single-digit millimeter range. Combined with the scanner's accuracy of less than 1 mm (see Table 2), an average deviation of 5 mm was considered as a representative maximum error. This error covers both the compounding accuracy of the scan and the accuracy of the determined hard points.

To investigate the effect of scan and node identification inaccuracies, the hard point coordinates of three main suspension components of the front axle have been altered. The toe and camber angle during compression and rebound have been chosen for comparison as these are two of the most influential characteristic kinematic values of a chassis.

The McPherson suspension, disregarding springing or elastic components, consists mainly of the wheel, steering knuckle, control arm, steering rod, and McPherson strut.

Since the initial toe, camber, and track width are defined separately in IPGKinematics, the wheel, steering knuckle, and their respective kinematic nodes have not been chosen for alteration, although the kingpin angle is defined by the nodes of the strut and control arm on the steering knuckle.

The tie rod end (TR), control arm/wishbone bushings (WBs) and the strut bearing (SB) have instead been chosen for alteration either on the vehicle body side (VB) or at the steering knuckle (SK). The length and mounting height and thus the control arm angle, as well as the angle at which the strut is mounted, directly influence the camber during rebound and compression, whereas the tie rod end position directly influences the toe-in during rebound and compression.

The effect of shifting one node 5 mm at a time in multiple directions is shown in Figure 8.

The resulting deviations depend on the observed angle. While changes to the tie rod in the z-direction have the greatest influence on the toe angle, as shown in Figure 8a, changes to the y-position of the strut bearings have the most significant impact on the camber angle, as shown in Figure 8b. However, the changes in the resulting wheel travel curves can still be considered minor overall.

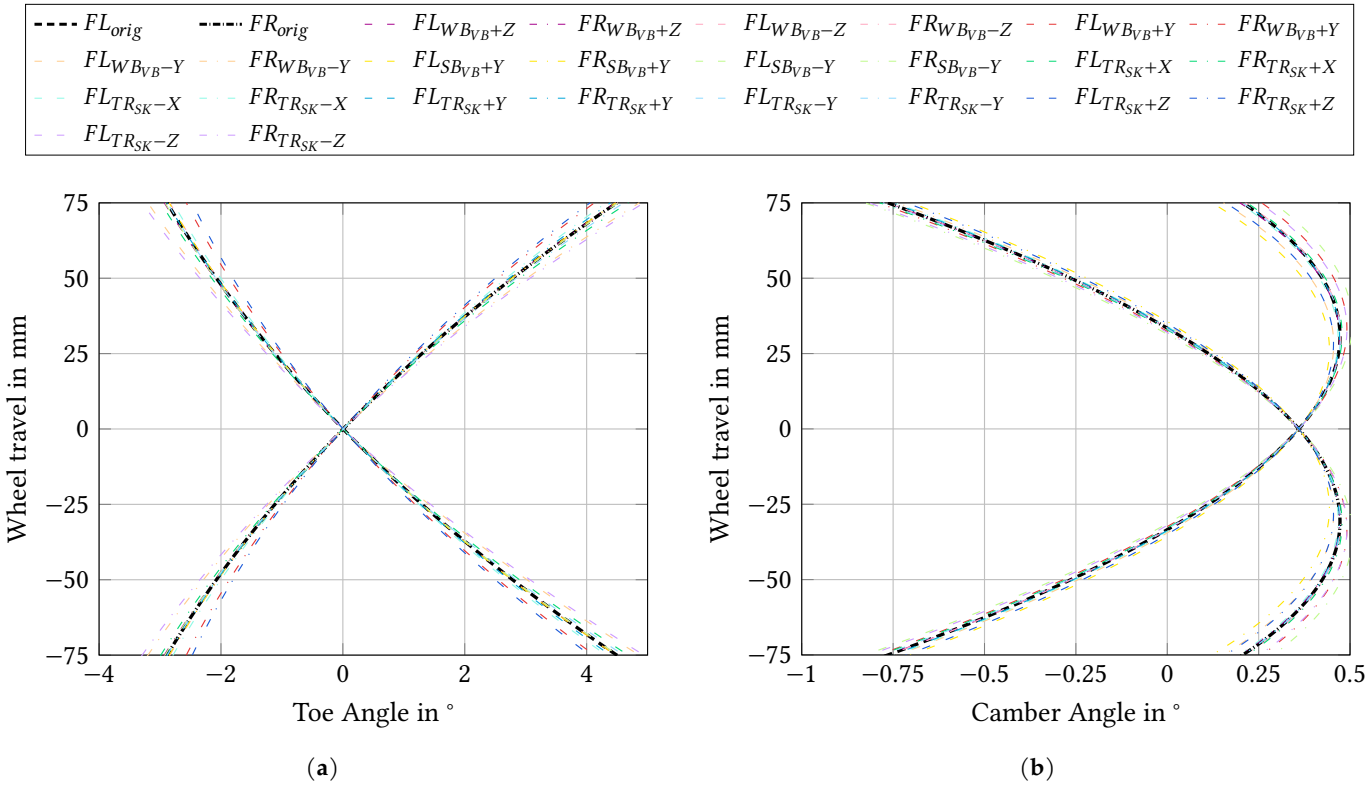


Figure 8. Wheel travel curves with slightly varied suspension kinematic parameters generated with CarMaker's Model Check functionality for both front wheels as a function of: (**a**) toe angle; (**b**) camber angle.

4.3. Application with CarMaker and Comparison with Road Test Data

Last, the resulting "Suspension Kinematics and Compliance" file from IPGKinematics was integrated into an example vehicle model in CarMaker Office 14.1.2. The example model was further modified based on the vehicle information in Table 1. In addition, a tire model matching the DUT was created using CarMaker's Tire Data Set Generator, and the powertrain was roughly adapted to all-wheel drive with the corresponding power and torque distribution. The tire model primarily influences the transferable forces and, together

with the drive force distribution, has a significant impact on the longitudinal and lateral accelerations occurring on the vehicle body. Finally, the values for the stabilizer bar and the springs on the front and rear axles were also estimated as linear models. The combination of these estimated subsystems has a dominant influence on the pitch and roll behavior.

To validate the simulation, additional test drives were conducted with the DUT on an outdoor test track. For this purpose, the DUT was equipped, among other things, with an IMU that measures body accelerations as well as pitch, roll, and yaw angles. A virtual IMU was also added to the simulation in the same location within the vehicle to enable a comparison of the results.

A circular drive with a constant diameter of 65 m was conducted both with the DUT and in the simulation. During this test, various velocities were reached and maintained so that a constant velocity and a constant steering angle could be set, thereby establishing quasi-stationary driving behavior. The velocity was gradually increased until just before the dynamic driving limit of the DUT. The circular drive was performed in both directions, resulting in both positive and negative accelerations. Due to an error in the measurement system of the DUT, the maximum value was not recorded during negative lateral acceleration in the real-world test. The results of the real-world test and the simulation can be compared in Figure 9. Figure 9a shows the velocity versus lateral acceleration, and Figure 9b shows the roll angle versus lateral acceleration.

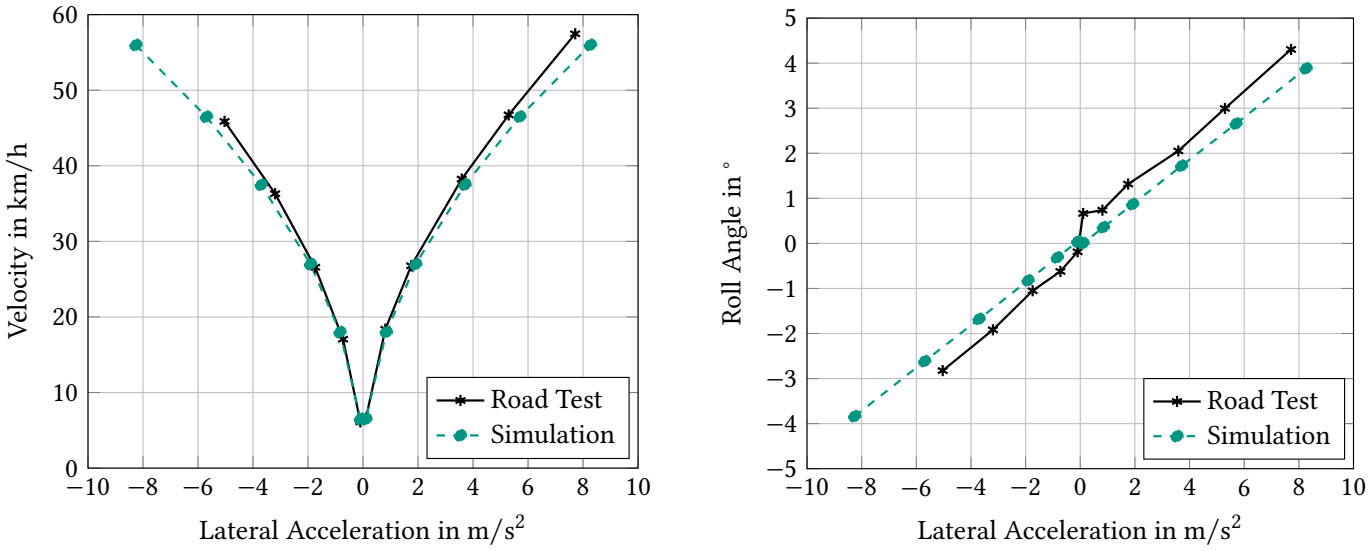


Figure 9. Comparison of road test and simulation data: (**a**) velocity over lateral acceleration; (**b**) roll angle relative to the lateral acceleration.

In simulation, the influence of the varied hard points discussed in Section 4.2 was also examined. Since the maximum deviation in the roll angle is approximately 0.025°, or 0.67 %, the results are not shown in Figure 9. These results also confirm the assertion made in Section 4.2 that deviations in the hard points can be neglected for the purposes of this paper.

Two observations from the real-world test are the slightly lower lateral acceleration at the same velocity compared to the simulation as well as the slightly larger roll angle in the real-world test. The difference in velocity between the simulation and the road test with the same lateral acceleration can still be considered good with a root mean squared error (RMSE) of 1.697 km/h and a coefficient of determination (R^2) of 0.989. The deviations in roll angle are more apparent, but, with an RMSE of 0.481° and an R^2 of 0.943, the accuracy is still within an acceptable range.

The possible causes for this include measurement inaccuracies in the IMU and insufficiently precise modeling of the vehicle. The example steering model has no influence here since, although a different steering wheel angle is set for the circular drive, only the wheel steering angle is relevant for the chassis model. However, the tire model, which was not modeled in detail, does have a direct influence on the wheel steering angle and thus the lateral acceleration and roll angle. In addition, the actual diameter of the driving circle had to be estimated using global navigation satellite system (GNSS) data. As a result, the radius in the simulation may differ slightly.

The lack of model accuracy is also the reason why the pitch angle as a function of longitudinal acceleration is not taken into account. To correctly simulate the pitch angle, the entire powertrain would also have to be accurately modeled in the simulation. Without this, the torque distribution would be incorrect, causing the vehicle to pitch differently. Furthermore, during higher acceleration, the tire model is also of importance.

Interpreting the yaw angle is also challenging as it depends not only on various vehicle parameters but also the IMU's position within the vehicle. An inaccurate determination of the IMU's position, which calculates the yaw angle for the real-world test, can lead to significant deviations in the yaw angle, thereby making the comparison more difficult.

5. Discussion

The application of the method presented in Section 3.3 in Sections 4.1–4.3 described above can be considered successful overall even though there are certain differences between the simulation results and the conducted tests under real-world conditions. These differences can be attributed to various causes, which are discussed in the following.

A closer analysis of the scanning process reveals several reasons. One major cause is the scanner's size, which prevented the scanning of certain objects, such as the front axle bearing. Added to this were shadowing effects as well as the lower accuracy compared to newer 3D scanners. Due to these challenges, objects and their positions could only be approximated during post-processing, meaning that assumptions had to be made when adding design elements. Although the influence of inaccurately determined hard points was investigated and found to be negligible, not all the hard points or combinations of different points were varied simultaneously due to the large number of possibilities. Furthermore, the exact wheel contact point was merely estimated as it was not clearly visible in the scan. The authors in [13] mention additional challenges in 3D scanning, such as surface reflections or different materials. One way to minimize the mentioned challenge is the disassembly of the entire chassis so that the individual components could be scanned separately. However, this would result in information loss regarding the design attitude. As an alternative, a compact depth camera was also used to access poorly accessible areas. However, the camera's resolution was too low to produce an adequate scan result.

In addition to the scanning process, determining the hard points from the point clouds and calculating the wheel travel curves in IPGKinematics involve uncertainties. The biggest challenge was determining the vehicle's longitudinal axis from the scan data in order to correctly extract the hard points. This requires a component that runs parallel to the vehicle's longitudinal axis. However, since most components in the chassis or on the vehicle's underbody are not aligned parallel to this axis or do not have straight contours, errors can occur when defining the vehicle's longitudinal axis. It is therefore advisable to integrate a longitudinally oriented feature into the scanning process itself. After the hard points have been successfully transferred to IPGKinematics, the next source of uncertainty in the data processing chain is the lack of elasticity data needed to generate the correct wheel travel curves. Elasticities always have an influence when accelerations act on the vehicle, including during quasi-stationary driving maneuvers such as driving in a circle. However,

the exact effect depends on the chassis and the maneuvers performed and therefore cannot be easily determined [25–27].

Finally, the other vehicle components mentioned in Section 4.3—which were inadequately modeled—also contribute to a deviation from the results of the real-world test. If the behavior of these components were known, the accuracy of the method could be estimated even more precisely and, for example, the influence of the hard points on the vehicle's exact body motion could be better assessed. Nevertheless, the approach provided good and usable results even though the effort required for the entire process is relatively high and can take several days from preparing the scan to running the simulation.

6. Conclusions and Outlook

This publication presents a method for generating a reliable chassis model without requiring extensive knowledge of the vehicle. Using a 3D scanner, one wheel from each of the front and rear axles was scanned, and the hard points of the chassis were determined from the scan. Based on these points, wheel travel curves were determined using the software IPGKinematics. These curves were applied in the CarMaker simulation environment and the vehicle's driving behavior was validated against real-world data of the DUT. Despite some simplifications, the results are promising and open up new possibilities for chassis analysis as well as driving dynamics simulations.

The generated chassis model is intended for future use on the ViL full-vehicle test bench shown in Figure 1 so that tests conducted on the test bench will be even more realistic. Theoretically, the DUT could also be scanned on the test bench after assembly. Without the tires, certain areas of the chassis would be better accessible and thus easier to scan. In this case, however, the tire contact point would have to be estimated.

To further optimize the described method, a different scanning procedure could also be used. In such an approach, unique adhesive dots—known as "tracker IDs"—are used instead of retroreflective dots. Each of these IDs has a unique pattern, allowing them to be unambiguously identified and enabling information to be stored in the scanning software for each ID or scanned component. This means, for example, that a pointing tool that has already been scanned can be used as an auxiliary tool for areas that are not accessible for the scanner. The scanner recognizes the tool based on the unique IDs on the pointing tool and can determine the position of the tool's end point using the stored information. If the end point touches a hidden area of the chassis and additional IDs on the chassis are visible to the scanner, a hard point can be precisely determined, which would otherwise only be estimated. Furthermore, poorly scanned areas or geometries could be reconstructed using artificial intelligence. Various use cases for artificial intelligence in combination with 3D scans are mentioned in [13].

A sensitivity analysis examining the impact of the determined model on the missing elasticities or the parameters assumed to be linear for the spring, damper, and stabilizer bar would also be interesting. A comprehensive comparison of the determined wheel travel curves could also be conducted by comparing them with results from a K&C test bench. Here, an additional cost–benefit analysis of the presented method compared to a K&C measurement could be conducted since the overall complexity of the presented method—and thus the time required—should not be underestimated and the necessary equipment, such as the scanner, must first be purchased. Last but not least, the method should also be applied to other vehicles and suspension variants.

Author Contributions: Conceptualization, P.R.; methodology, P.R. and N.L.O.; software, P.R. and N.L.O.; validation, P.R. and N.L.O.; formal analysis, P.R. and N.L.O.; investigation, P.R. and N.L.O.; resources, P.R. and N.L.O.; data curation, P.R. and N.L.O.; writing—original draft preparation, P.R. and

N.L.O.; writing—review and editing, P.R., N.L.O. and M.F.; visualization, P.R. and N.L.O.; supervision, M.F. All authors have read and agreed to the published version of the manuscript.

Funding: This research received no external funding.

Institutional Review Board Statement: Not applicable.

Data Availability Statement: The datasets presented in this article are not readily available because the paper primarily focuses on the methodology itself rather than the data used, which is not relevant to the general application of this methodology. Furthermore, the data is largely product-specific, and the authors cannot share the data without the consent of the manufacturer and the vehicle owner. Requests to access the datasets should be directed to the correspondence author.

Acknowledgments: The authors would like to thank APL Automobil-Prüftechnik Landau GmbH (Germany) for providing the test vehicle.

Conflicts of Interest: The authors declare no conflicts of interest.

Abbreviations

The following abbreviations are used in this manuscript:

3D	Three-dimensional
CAD	Computer-aided design
COG	Center of gravity
DUT	Device under test
GNSS	Global navigation satellite system
IMU	Inertial measurement unit
K&C	Kinematics and compliance
KIT	Karlsruhe Institute of Technology
MBS	Multi-body system
R^2	Coefficient of determination
RMSE	Root mean squared error
SB	Strut bearing
SK	Steering knuckle
TR	Tie rod end
VB	Vehicle body side
ViL	Vehicle-in-the-loop
WB	Wishbone bushing

References

1. Rautenberg, P.; Reick, B.; Engelmann, D.; Frey, M.; Gauterin, F. Battery Electric Vehicle-in-the-Loop Power and Efficiency Measurement Test Method. *SAE Int. J. Adv. Curr. Pract. Mobil.* **2023**, *6*, 1925–1935. [CrossRef]
2. Rautenberg, P.; Piecha, P.; Frey, M.; Pfister, F. Testing of ADAS Functions on a Steerable ViL Full Vehicle Test Bench. *ATZ Worldw.* **2026**, *128*, 42–47. [CrossRef]
3. Piecha, P.; Rautenberg, P.; Friedmann, M. Optimized Merging of the Virtual World and Reality on the Vehicle-in-the-Loop Test Bench. In Proceedings of the 33. Aachen Colloquium Sustainable Mobility, Aachen, Germany, 7–9 October 2024. [CrossRef]
4. Solmaz, S.; Holzinger, F. A Novel Testbench for Development, Calibration and Functional Testing of ADAS/AD Functions. In Proceedings of the 2019 IEEE International Conference on Connected Vehicles and Expo (ICCVE), Graz, Austria, 4–8 November 2019. [CrossRef]
5. Förster, M.; Hettel, R.; Schyr, C.; Pfeffer, P.E. Lateral dynamics on the vehicle test bed—A steering force module as a validation tool for autonomous driving functions. In Proceedings of the 9th International Munich Chassis Symposium 2018, Wiesbaden, Germany, 25 September 2018. [CrossRef]
6. Schmelzle, M.H.; Robinette, D.L.; Bos, J.P. Tire-force modeling on a hub-mounted vehicle-in-the-loop dynamometer while performing lateral maneuvers. In *Proceedings of the SPIE Defense + Security Conference, Orlando, FL, USA, 13 June 2023*; Autonomous Systems: Sensors, Processing, and Security for Ground, Air, Sea, and Space Vehicles and Infrastructure; SPIE: Nuremberg, Germany, 2023. [CrossRef]
7. Paulweber, M.; Lebert, K. *Mess- und Prüfstandstechnik: Antriebsstrangentwicklung·Hybridisierung·Elektrifizierung*; Springer Fachmedien: Wiesbaden, Germany, 2014. [CrossRef]
8. Kurz, C.; Stangenberg, L.; Gauterin, F. A Generic Approach to Modeling Vehicle Pitch Dynamics on a Vehicle Test Bench. *IEEE Open J. Veh. Technol.* **2023**, *4*, 739. [CrossRef]

9. Zeitvogel, D.; Ahlert, A.; Neubeck, J.; Krantz, W.; Wiedemann, J.; Boone, F.; Kan, W. An Innovative Test System for Holistic Vehicle Dynamics Testing. In *Proceedings of the WCX SAE World Congress Experience, Detroit, MI, USA, 9 April 2019*; SAE Technical Paper; SAE International: Warrendale, PA, USA, 2019. [CrossRef]
10. Zeitvogel, D.; Krantz, W.; Neubeck, J.; Wagner, A. Holistic vehicle parametrization on a handling roadway. *Automot. Engine Technol.* **2022**, *7*, 209–216. [CrossRef]
11. Sović, L.; Bušić, M.; Muminović, A.J.; Trobradović, M. Application of 3D Scanning in the Automotive Industry. In *Proceedings of the International Symposium on Innovative and Interdisciplinary Applications of Advanced Technologies, Sarajevo, Bosnia and Herzegovina, 19–22 June 2026*; Advanced Technologies, Systems, and Applications X; Springer Nature: Cham, Switzerland, 2026; pp. 617–633. [CrossRef]
12. Othman, S.A.T.; Azman, A.H.; Wahid, Z.; Azman, M.A. Reverse Engineering of Brake Calliper Design via Integration of Topology Optimisation and Lattice Structure for Additive Manufacturing. *J. Kejuruter.* **2024**, *36*, 439–446. [CrossRef] [PubMed]
13. Debnath, B.; Pourfarash, Z.; Ghorpade, B.; Raman, S. Integrating Reverse Engineering for Digital Model Reconstruction and Remanufacturing of Mechanical Components: A Systematic Review. *Metrology* **2025**, *5*, 66. [CrossRef]
14. Freddi, M.; Ferretti, P.; Alessandri, G.; Liverani, A. Reverse Engineering of a Racing Motorbike Connecting Rod. *Inventions* **2023**, *8*, 23. [CrossRef]
15. Zhang, H.B.; Chang, Y.; Zhang, R.J.; Fan, H.Y. Reverse Modeling of Vehicle Suspension Control Arm. *Appl. Mech. Mater.* **2013**, *427–429*, 1183–1186. [CrossRef]
16. Matei, L.; Dumitru, I.; Racila, L.; Racila, M.; Tutunea, D.; Otat, O. Construction of a Kart Chassis Through 3D Reconstruction Methods—Part 2—Reverse Engineering. In Proceedings of the 30th SIAR International Congress of Automotive and Transport Engineering, Craiova, Romania, 23 October 2020. [CrossRef]
17. Ersoy, M.; Gies, S.; Prokop, G.; Schimmel, C. (Eds.) *Fahrwerkhandbuch: Grundlagen—Fahrdynamik—Fahrverhalten–Fahrwerkkomponenten—Elektronische Systeme—Fahrerassistenz—Autonomes Fahren—Entwicklungsprozesse—Perspektiven*; ATZ/MTZ-Fachbuch; Springer Fachmedien: Wiesbaden, Germany, 2026. [CrossRef]
18. Heißing, B.; Ersoy, M. (Eds.) *Chassis Handbook*; Vieweg+Teubner: Wiesbaden, Germany, 2011. [CrossRef]
19. Barton, D.C.; Fieldhouse, J.D. *Automotive Chassis Engineering*; Springer International Publishing: Cham, Switzerland, 2024. [CrossRef]
20. Schramm, D.; Kracht, F.E.; Sieberg, P.M. *Modellbildung und Simulation der Dynamik von Kraftfahrzeugen*; Springer: Berlin/Heidelberg, Germany, 2025. [CrossRef]
21. Liu, C.; Zhang, Y.; Deubel, C.; Kocksch, F.; Kubenz, J.; Prokop, G. Identification of Kinematic Points Based on KnC Measurements from the Suspension Motion Simulator. In *Proceedings of the IAVSD International Symposium on Dynamics of Vehicles on Roads and Tracks, Gothenburg, Sweden, 12–16 August 2019*; Advances in Dynamics of Vehicles on Roads and Tracks; Springer Nature Switzerland: Cham, Switzerland, 2019; pp. 1786–1793. [CrossRef]
22. Liu, C.; Zhou, J.; Gerhard, A.; Kubenz, J.; Prokop, G. Characterization of the Vehicle Roll Movement with the Dynamic Chassis Simulator. In Proceedings of the Vehicle and Automotive Engineering Conference, Miskolc, Hungary, 23–25 May 2018. [CrossRef] [PubMed]
23. Go!SCAN 3D. Available online: https://go.creaform3d.com/lp-goscan-3d-fm?utm_source=google&utm_medium=cpc&utm_campaign=20.90.1.0-BRANDED-Search-DACH-EN&gad_source=1&gad_campaignid=12066288172&gclid=EAIaIQobChMIk6r29NHjlQMVzKhoCR0CDjpaEAAYASAAEgKpBvD_BwE (accessed on 10 September 2026).
24. IPG Automotive. *IPGKinematics Reference Manual*, Version 3.6.11.1; 2022.
25. Kracht, F.; Unterreiner, M.; Schramm, D. Einfluss von Elastizitäten in Fahrwerken auf die Fahrdynamik—Influence of elasticities in chassis on vehicle dynamics. In Proceedings of the Fachtagung Mechatronik 2015, Dortmund, Germany, 12–13 March 2015. [CrossRef]
26. Kracht, F.E. Modellbildung und Simulation der Dynamik und Elastokinematik von Radaufhängungen für Echtzeitanwendungen. Ph.D. Thesis, Universität Duisburg-Essen, Duisburg, Germany, 2020. [CrossRef] [PubMed]
27. Büchner, S. Einfluss Elastokinematischer Achskennwerte auf die Fahrdynamik. Ph.D. Thesis, Technische Universität München, Munich, Germany, 2020.

Disclaimer/Publisher's Note: The statements, opinions and data contained in all publications are solely those of the individual author(s) and contributor(s) and not of MDPI and/or the editor(s). MDPI and/or the editor(s) disclaim responsibility for any injury to people or property resulting from any ideas, methods, instructions or products referred to in the content.